

## SIMULTANEOUS MEASUREMENTS OF PARTICLE SIZE AND VELOCITY WITH SPATIAL FILTERING TECHNIQUE IN COMPARISON WITH COULTER MULTISIZER AND LASER DOPPLER VELOCIMETRY

D. PETRAK

Department of Technical Thermodynamics,  
Chemnitz University of Technology, Germany

**Abstract-** The objective of this study is to compare the measuring results of an optical probe based on a modified spatial filtering technique with given size distributions of different test powders and also with particle velocity values of laser Doppler measurements. Fibreoptical spatial filtering velocimetry was modified by fibreoptical spot scanning in order to determine size of particles. Test particles were narrow sized glass beads in the range of 30  $\mu\text{m}$  to 100  $\mu\text{m}$ . Limestone particles in the range of 10  $\mu\text{m}$  to 600  $\mu\text{m}$  have been used for the particle velocity measurements with a laser Doppler velocimeter. Particles were dispersed by a brush disperser and the size or velocity measurements were carried out in a free particle laden air stream. Probe results are corresponding with the given test particle sizes and with the laser Doppler velocity values.

*Key words:* probe technique, in-line particle sizing, particle velocity, test measurements

### 1. INTRODUCTION

Sizing of particles in industrial processes is of great technical interest and therefore different physical-based techniques have been developed (Allen 1997). Especially in-line measurement techniques may provide a better understanding of the phenomena in particle systems and also improve the control of processes. Advantages are then the improvement of the process stability and of the product quality and otherwise the reduction of waste, store and costs. Another interesting parameter is the particle velocity in particle laden flows or in particulate materials. The simultaneous measurement of size and velocity of each particle allows the determination of the particle mass flow rate as an important value of the particle flow.

Particle size measurement techniques are divided into two categories, stream scanning and field scanning. Stream scanning means the examination of one particle at a time and field scanning the simultaneous examination of an assembly of particles. Both principles may applied on particle sizing of industrial processes, making on-line size analysis. Inserting a probe directly into a process line is called in-line particle sizing. Ideally, the whole process flow would be examined, but process streams often operate at high particle flow rates. It is therefore preferable to measure in a side-stream which can be isolated from the main process flow. Another addition is the application of a dilution step between the particle stream and the measuring device.

Known in-line measuring devices based on field scanning use the laser diffraction, incoherent space frequency analysis and ultrasonic or light attenuation. The application of the laser diffraction method requires large effort in industrial process examination (Witt and

Röthele 1998). Sachweh et al (1998) have developed a new light scattering method for in-line measurement of mean particle sizes in suspensions and Feller et al (1998) use a combined measurement of backscattering and extinction.

Examples of in-line sizing devices based on stream scanning are the focused beam reflectance determination, the shadow Doppler technique, light scattering, imaging technique using CCD cameras, the phase Doppler method (PDA) and a modified spatial filtering technique. The PDA method needs optically homogeneous spheres with known complex refractive indices. There is a lot of work to develop the PDA in relation to inhomogeneity and absorptivity of the particle medium. New results show that the PDA requires a priori knowledge of optical properties (Wriedt et al 1993, Köser and Wriedt 1996, Schneider and Hirleman 1994, Onofri et al 1996). Naqwi and Fandrey (1997) have developed a PDA technique to measure the size of irregular particles smaller than 20  $\mu\text{m}$ .

Hardalupas et al (1994), Morikita et al (1994, 1995) and Morikita (1996) have developed the shadow Doppler velocimetry (SDV) to measure the size of irregular, opaque particles. The SDV is based on the combination of a particle imaging technique and the well known laser Doppler velocimetry (LDV). Morikita and Taylor (1998) have shown the ability of the SDV technique to size optically inhomogeneous particles of a water-based paint spray, as used in industrial coating processes. The application of the SDV is limited to measurements in processes with a small particle number density. Another disadvantage of the SDV is the forward scattering technique.

Based on a modified spatial filtering technique Petrak et al (1996, 1998) have presented a new optical probe for the simultaneous measurement of size and velocity at one particle. Fibreoptical spatial filtering velocimetry was modified by fibreoptical spot scanning in order to determine the particle size. Meanwhile an in-line measuring device with the probes IPP30 and IPP50 based on modified spatial filtering technique is available by PARSUM (1999). The advantages of this in-line measuring device are the low hardware requirements, the user friendly handling, long time stability and the robust design at reasonable invest costs.

The purpose of the present work was to demonstrate the accuracy of the size and velocity measurements by using the modified spatial filtering technique and by using a laser Doppler velocimeter (LDV) and narrow classified test powders characterized by measurements with a Coulter multisizer.

## 2. MEASURING PRINCIPLE

The spatial filtering velocimetry (SFV) is a method of determining the velocity of an object by observing the object through a spatial filter in front of a receiver. An overview about the SFV method was given by Aizu and Asakura (1987). The modified spatial filtering technique for the simultaneous measurement of particle size and velocity can be described as follows.

The fibreoptical spot scanning (FSS) is an addition to the SFV. The basic operation of the FSS is to observe the shadow image of a moving particle through a single optical fibre with a small diameter  $d$ . When the shadow image passes through the single optical fibre, an impulse is generated the width of which depends on the particle size  $x$ , the particle velocity  $v$  and the location of particle and fibre. The composition of the total impulse width is shown in figure 1. The total time  $\Delta t$  of the impulse is then:

$$\Delta t = (t_2 - t_1) + (t_3 - t_2) + (t_4 - t_3) = (d/v) + ((x-d)/v) + (d/v) \quad [1]$$

and the particle size is equal

$$x = v (t_2 - t_1) = v (t_4 - t_3) = v \cdot \Delta t - d \quad [2]$$

Equation (2) is valid too, if the particle is smaller than the diameter  $d$  of the single fibre. According to figure 2 the particle trajectory has a random position in relation to the spatial fixed single fibre. If the particle is a sphere with the radius  $r$  then the result is a distribution of chord lengths  $a(y)$  of the shadow image of the particle:

$$a = 2\sqrt{2hr - h^2} \quad , \quad a(y) = 2\sqrt{2r(r - y) - (r - y)^2} \quad [3]$$

with  $y$  as the distance of the chord from the  $x$ -axis.

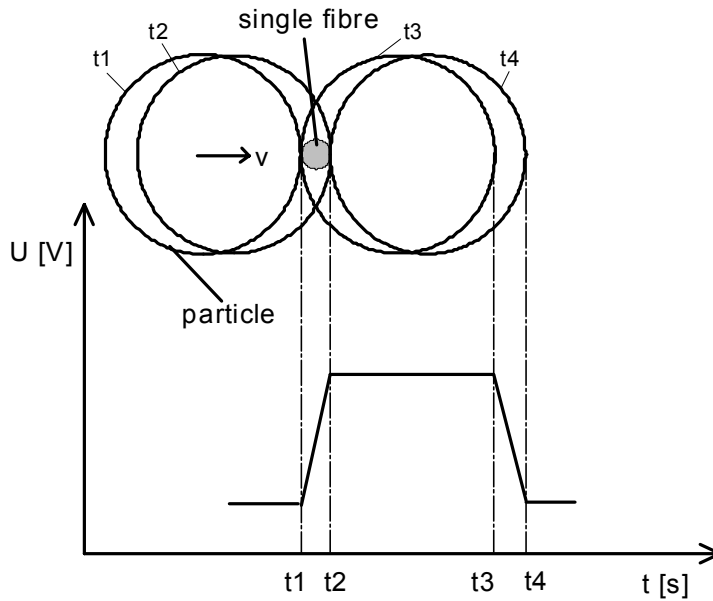


Figure 1. Impuls generation by fibreoptical spot scanning

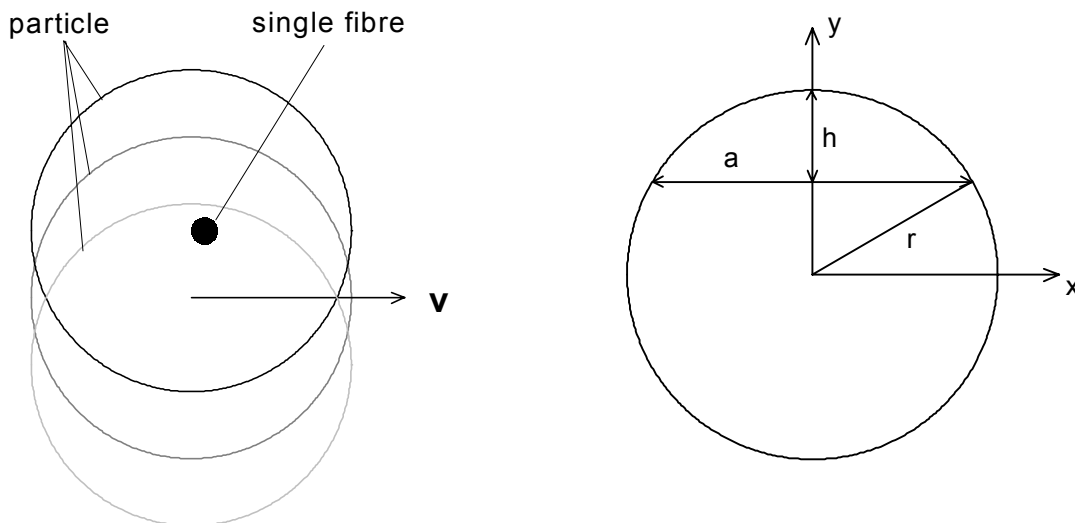


Figure 2. Random particle position and random chord length determination

The SFV is used to determine the unknown particle velocity  $v$ . As mentioned above the basic operation of SFV is to observe the image of a moving object through a spatial filter placed in

front of a photodetector. The output signal of the photodetector contains a frequency  $f_o$  related to the object velocity  $v$ :

$$v = f_o \cdot g / M, \quad [4]$$

where  $g$  is the interval of the spatial filter and  $M$  is the magnification of the imaging system. Various types of spatial filtering velocimeter are mainly characterised by the physical types of the spatial filter: transmission grating type, detector type, optical fibre type, and special grating type. The optical fibre type was investigated by Hayashi and Kitigawa (1982).

The probe with the modified spatial filtering technique uses a fibreoptical configuration which is demonstrated in figure 3. The single fibre for spot scanning and a fibreoptical spatial filter are arrayed together. Optical fibres of diameter  $a$  are linearly arrayed at intervals of  $g/2$ . The shadow of a moving particle is formed at the entrance faces of a differential-type optical fibre spatial filter with the interval  $g$ . The output light from every other fibre is collected, and an output signal is obtained by taking the difference between them to eliminate the pedestal frequency around zero spatial frequency.

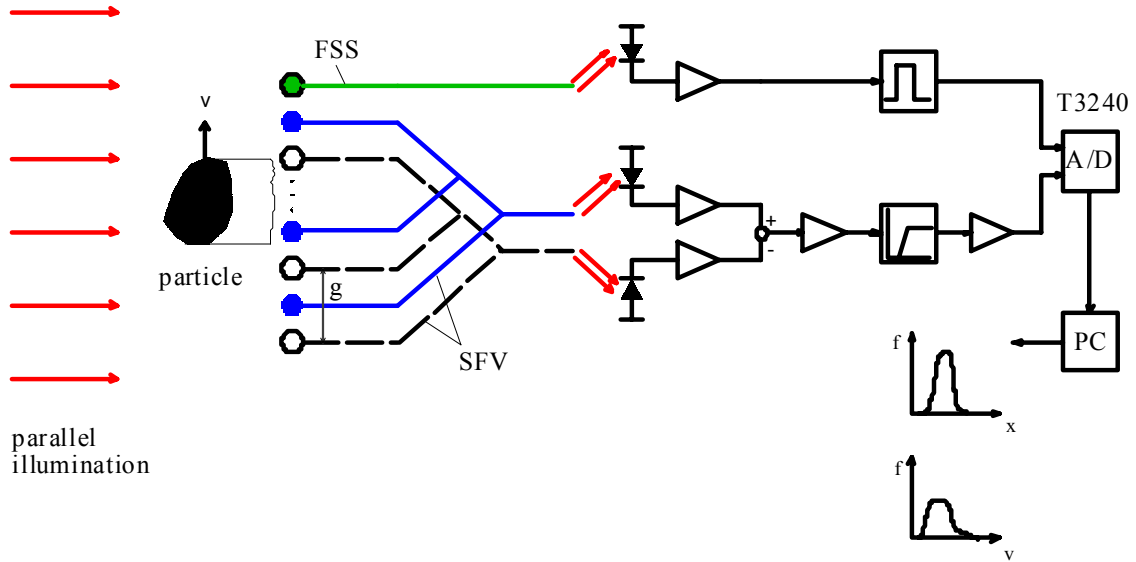


Figure 3. Schematic diagram of the modified spatial filtering technique

The power spectrum  $H(\mu, \nu)$  of the spatial filter function represents the selective characteristic in the spatial frequency domain. It can be obtained by Fourier transforming after weighting  $\pm 1$  at the end faces of uniform optical fibres:

$$|H(\mu, \nu)|^2 = \pi^2 a^4 (\sin \pi g \mu / 2)^2 \left( \frac{\sin N \pi g \mu}{\sin \pi g \mu} \right)^2 \left( \frac{J_1(\pi a \sqrt{\mu^2 + \nu^2})}{\pi a \sqrt{\mu^2 + \nu^2}} \right)^2, \quad [5]$$

where  $\mu$  and  $\nu$  are the spatial frequencies in the  $x$  and  $y$  directions, respectively,  $J_1$  is the Bessel function of the first order, and  $2N$  is the total number of the fibres. According to equation (5), the optical fibre array selects a narrowband spatial frequency around  $\mu = 1/g$  and acts as a filtering function on the input function  $F_p(\mu, \nu)$  in the space domain. The spatial power spectral density function  $G_p(\mu, \nu)$  is given by:

$$G_p(\mu, \nu) = F_p(\mu, \nu) |H(\mu, \nu)|^2, \quad [6]$$

where  $F_p(\mu, \nu)$  stands for the Fourier transform of the image intensity  $f(x, y)$ . The temporal power spectral density function  $G_p(f)$  is given by integrating (6) with respect to the spatial frequency  $\nu$ :

$$G_p(f) = \frac{1}{\nu} \int_{-\infty}^{\infty} F_p\left(\frac{f}{\nu}, \nu\right) \left|H\left(\frac{f}{\nu}, \nu\right)\right|^2 d\nu, \quad [7]$$

where a relation of  $\mu = f/\nu$  has been used. The temporal power spectrum  $G_p(f)$  may have a peak at  $f = f_o = \nu/g$ . By measuring the frequency  $f_o$ , the particle velocity  $\nu$  can be determined from equation (4).

The spatial filter should be constructed to have the appropriate filtering characteristics by choosing the following parameters: transmittance, interval of filter elements, number of filter elements. A systematic deviation smaller than 1 % of the central frequency  $f_o$  is almost negligible for the number of filter elements  $N > 5$ . The visibility of the output signal depends on ratio shadow size  $x$  to interval  $g$ . A high visibility is obtainable for  $x/g$  less than 0.5. The optical fibres have an insufficiently long aperture size in the direction perpendicular to the spatial filter axis. Therefore, the proposed method is not qualified for chaotic particle movement.

Various signal-analysing techniques used in laser Doppler anemometry can also be used in spatial filtering velocimetry: spectrum analysis, correlation, frequency counting, and frequency tracking.

### 3. INSTRUMENTATION AND EXPERIMENTAL APPARATUS

#### 3.1 Instrumentation

The optical unit and signal processing are illustrated in figure 3. The illumination unit, the fibreoptical unit and the electronics are arrayed in a measuring probe with a cylindrical measuring pipe made by stainless steel (figure 4).

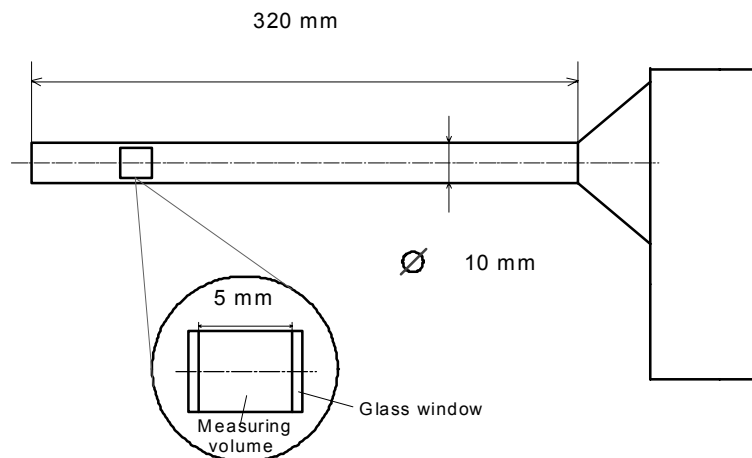


Figure 4. Schematic view of the measuring probe

The measuring pipe has a diameter of 10 mm and the measuring volume is arrayed at a distance of 32 mm from the top. The illumination unit is located left from the measuring volume and the fibreoptical unit right. Both optical units are protected by special glass windows.

Two different illumination units are used to generate a parallel light beam with high optical power. The first illumination unit contains a high-performance LED (fibre-coupled power 150  $\mu$ W, wavelength 810 nm) coupled with a short fibre and a graded index lens. The second illumination unit is a laser diode module (output power 3 mW, wavelength 670 nm) combined with an objective. The spatial filter is made by  $2N = 18$  step index fibres (core diameter 125  $\mu$ m, cladding 140  $\mu$ m) and the single fibre by a step index fibre with 28  $\mu$ m core diameter. The measuring volume has a size of 1.76 mm<sup>3</sup>. The photodetectors are Si-PIN-photodiodes with 1 mm<sup>2</sup> photosensitive area. Signal processing is realized by a two-channel 40 MHz transient recorder card T 3240. In order to obtain the central frequency  $f_0$  in equation (4), the Fast Fourier Transform (FFT) was applied. The magnification  $M = 1$  is valid for the particle shadow projection with a parallel light beam. Using a trigger unit to get a TTL-impulse in the single size channel, the total time in equation (3) was determined by counting the number of samples. In order to obtain a high accuracy, the sampling frequency of the size channel is much higher than the sampling frequency of the velocity channel. The first part of the signal processing is the signal validation to select a valid particle event. The measurement begins with a particle event in the size channel and after that, the validation of the velocity signal follows. The result is an array with the velocity and size values for each measured particle. These values are used for different statistical analysis: especially number size distribution, volume size distribution and velocity distribution. Both signals of one particle are illustrated in figure 5.

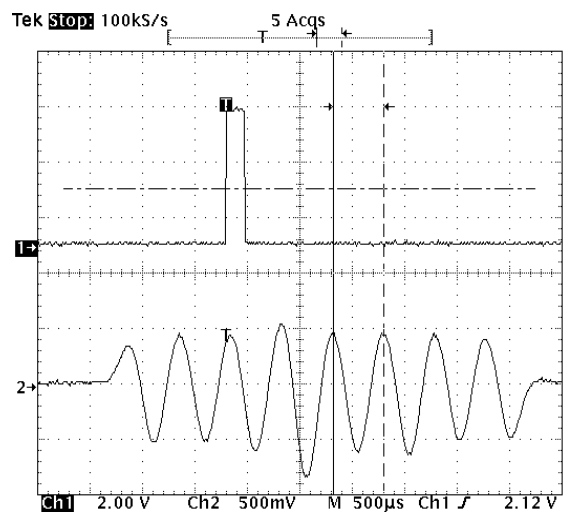


Figure 5. Output signals of a single particle : upper signal – size impuls with  $x = 80 \mu\text{m}$   
 lower signal – burst with  $v = 0.58 \text{ m/s}$

### 3.2 Experimental apparatus

Figure 6 shows the experimental setup. The particles were dispersed by a powder brush disperser RBG-1000 from PALAS and the air-particle flow was feeded into a horizontal pipe with an inner diameter of 15 mm. The volume flow of the compressed air has to be set constant. The measuring volume of the probe and the LDV was laid at the same position 50 mm away from the pipe outlet in the region of the free air-particle jet. A single-component laser Doppler velocimeter (Model LDV-380, Polytec, Germany) with a receiver for the backward scattered laser light allowed the determination of the particle velocities inside of the

free jet. The system incorporated a 100 mW laser diode. The measuring volume is characterized by a measuring volume of  $180 \times 180 \times 1900 \mu\text{m}^3$  and  $4.3 \mu\text{m}$  fringe distance.

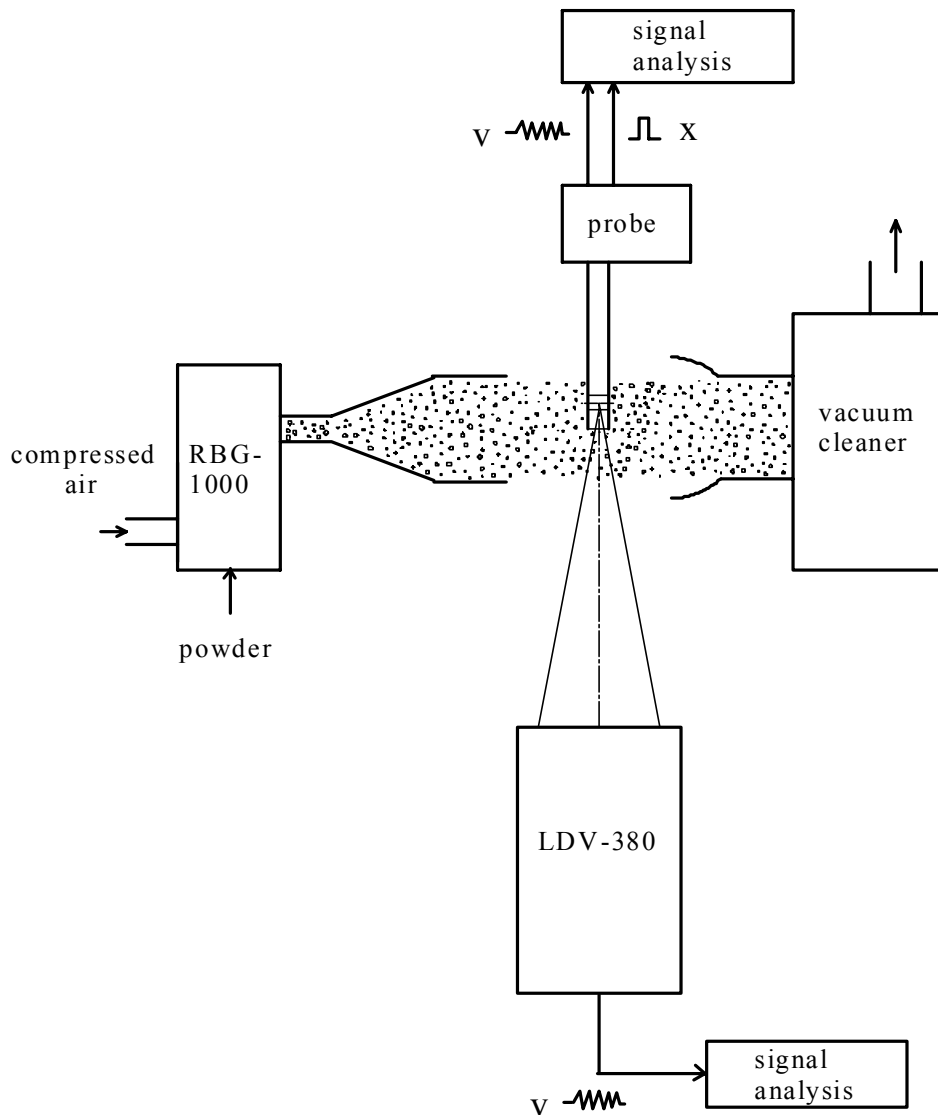


Figure 6. Experimental setup

According to the size measurements the test powders were three glass beads fractions made by APPIE, the Association of Powder Process Industry & Engineering of Japan, with narrow size distributions:

GBL30:  $x_{10} = 26 \mu\text{m}$ ,  $x_{50} = 30 \mu\text{m}$ ,  $x_{90} = 34$ ,

GBL60:  $x_{10} = 55 \mu\text{m}$ ,  $x_{50} = 59 \mu\text{m}$ ,  $x_{90} = 63 \mu\text{m}$ ,

GBL100:  $x_{10} = 97 \mu\text{m}$ ,  $x_{50} = 100 \mu\text{m}$ ,  $x_{90} = 105 \mu\text{m}$ .

The particle size distributions were measured by Coulter multisizer and in addition by a laser diffraction system HELOS from Sympatec. Size measurements by the probe were carried out at very low particle loading in order to compare the results with calculated chord length distributions for a single spherical particle. Limestone particles from type eskal made by KSL company were used for the velocity measurements with the following sizes:

eskal 10:  $x_{10} = 13 \mu\text{m}$ ,  $x_{50} = 21 \mu\text{m}$ ,  $x_{90} = 29 \mu\text{m}$ ,  
eskal 80:  $x_{10} = 58 \mu\text{m}$ ,  $x_{50} = 70 \mu\text{m}$ ,  $x_{90} = 84 \mu\text{m}$ ,  
eskal 0.1-0.5:  $x_{10} = 107 \mu\text{m}$ ,  $x_{50} = 295 \mu\text{m}$ ,  $x_{90} = 583 \mu\text{m}$ .

Glass beads and limestone particles are shown in the figures 7 and 8.

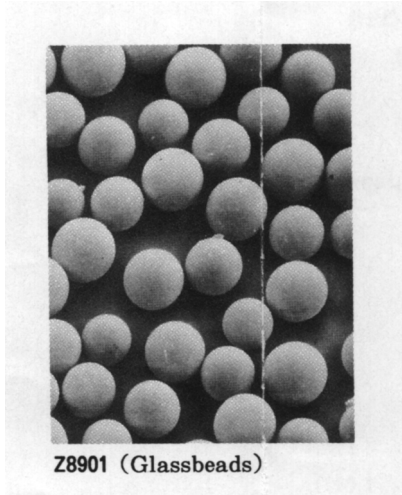


Figure 7. glass beads, APPIE

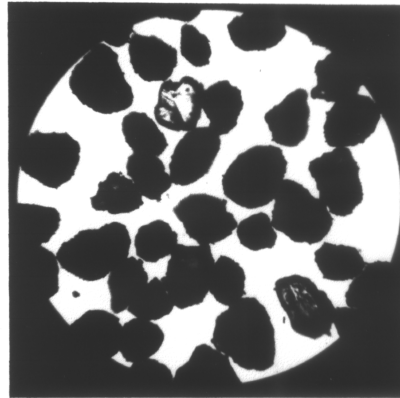


Figure 8. Limestone particles eskal80, KSL

## 4. RESULTS AND DISCUSSIONS

### 4.1 Particle size

In figure 9, density distributions  $q_{0,lg}(x)$  of the chord length distribution for a sphere with  $100 \mu\text{m}$  diameter are plotted against a logarithmic abscissa  $x$ . The determination was carried out both for the calculation model according equation (3) and for the measuring values of the glass bead fraction GBL 100. Following assumptions are valid for the calculation model:

- every particle position has the same probability,
- every particle has the same velocity,
- every particle has a constant diameter of  $100 \mu\text{m}$ .

In both cases the number of particles was greater than 1000. The measurements were controlled by an oscilloscope in order to proof the one particle regime. It can be seen that the two density distributions correspond very well. Differences at particle sizes greater than  $100 \mu\text{m}$  are caused by the fixed diameter of the model and otherwise by amounts of particles greater than  $100 \mu\text{m}$  for GBL 100.

In figure 10, density distributions  $q_{0,lg}(x)$  of the glass beads GBL 100 are shown for the Coulter mustersizer results and also for the probe results. The influence of the chord model and also a small amount of particle coincidence near to  $100 \mu\text{m}$  can be seen.

Figure 11 and 12 show the experimental results for the three glass bead fractions GBL 30, GBL 60 and GBL 100. The cumulative distributions  $Q_3(x)$  and the density distributions  $q_{3,lg}(x)$  are shown comparatively. It can be seen that the modified spatial filter technique can distinguish clearly the different size fractions. Using the  $Q_{3,50}$ -values the differences to the corresponding Coulter mustersizer values are as follows: GBL 30: +10 %, GBL 60: -8 %, GBL 100: + 3 %. As expected the results of the probe measurements show a broader size distribution caused by the statistical measurement of the cord length's of glass beads. Nevertheless there is a good agreement between both size distributions (modified spatial filter technique and Coulter mustersizer) with a maximal difference of 10 %.



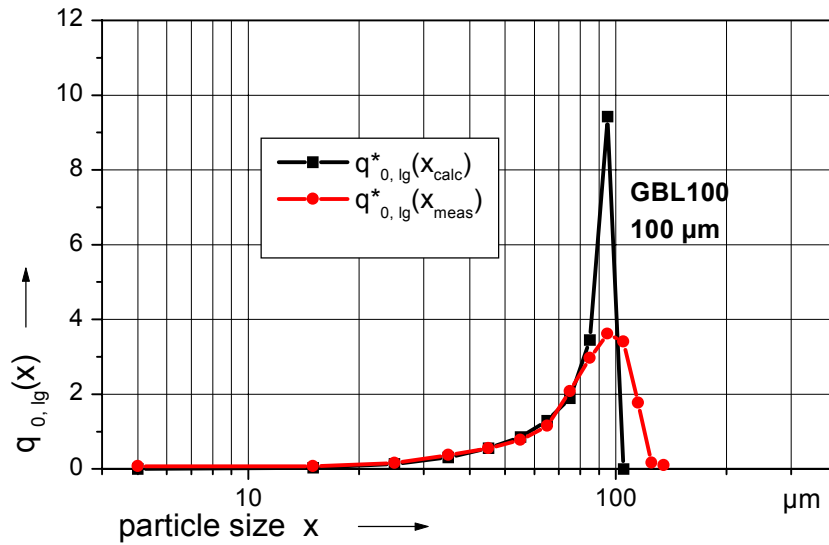


Figure 9. Density distributions  $q_{0,lg}(x)$  of the chord length for one sphere and GBL 100 Model and probe measurement

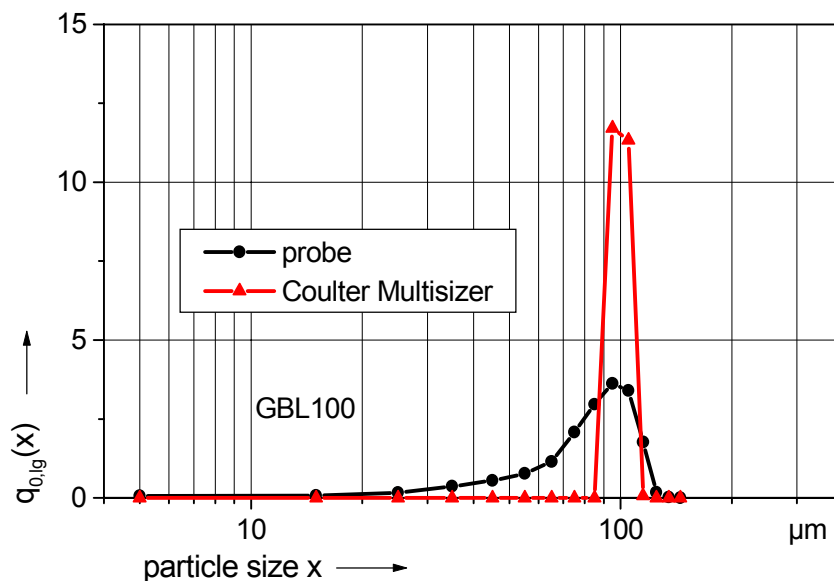


Figure 10. Density distributions  $q_{0,lg}(x)$  of experimental results for GBL 100 Probe and Coulter multisizer measurements

#### 4.2 Particle velocity

CFD results of Hussainov (1999) show a symmetrical flow inside the measuring volume of the probe with a velocity difference of maximal +10 % to the surrounding flow. The horizontal velocities of about 2000 particles were measured at the same spatial position by the LDV and by the probe. Results are shown in the figures 13 and 14 for the limestone fractions eskal 20 and eskal 80. As expected the particle velocity distributions measured by the probe are a little broader than the distributions measured by the laser Doppler velocimeter. This effect is caused by the wall contact of the particles with the probe and therefore smaller velocities are increased or do now exist. The mean velocities measured by the probe are about

6 % smaller than the same values measured by the LDV and the standard deviations are doubled. This decreasing effect has no influence on correct particle sizing.

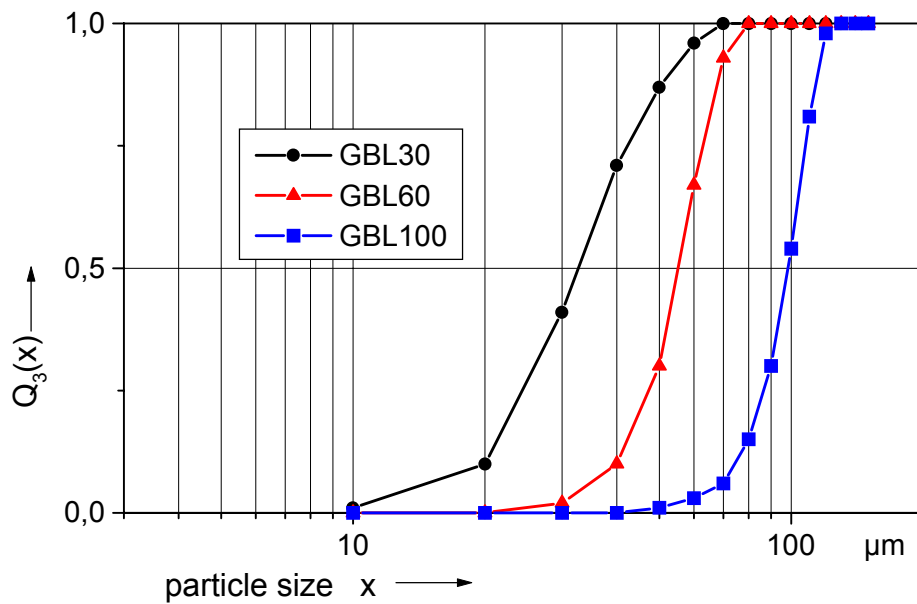


Figure 11. Cumulative distributions for glass beads GBL 30, GBL 60 and GBL 100 measured by probe

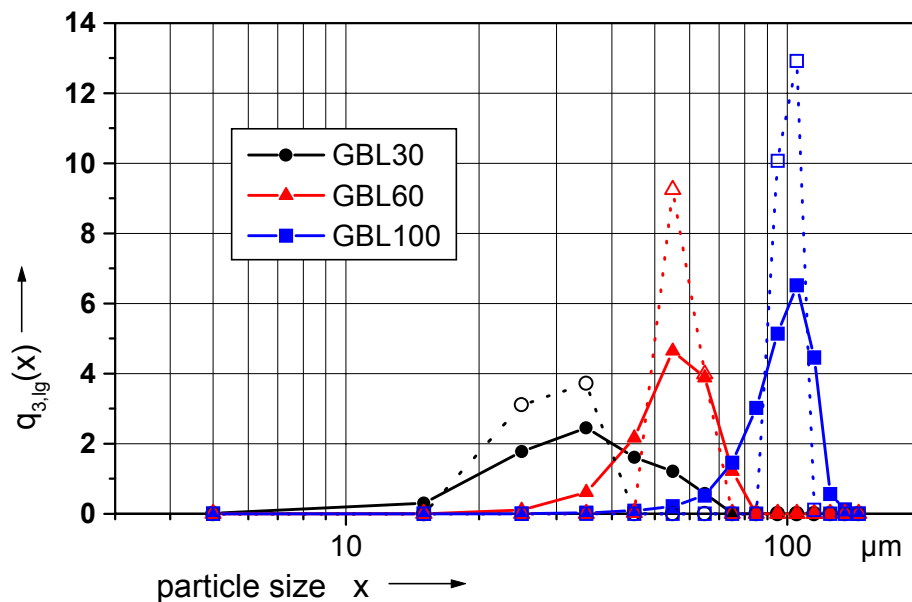


Figure 12. Density distributions for glass beads GBL 30, GBL 60 and GBL 100 dotted lines: Coulter mastersizer, regular lines: probe

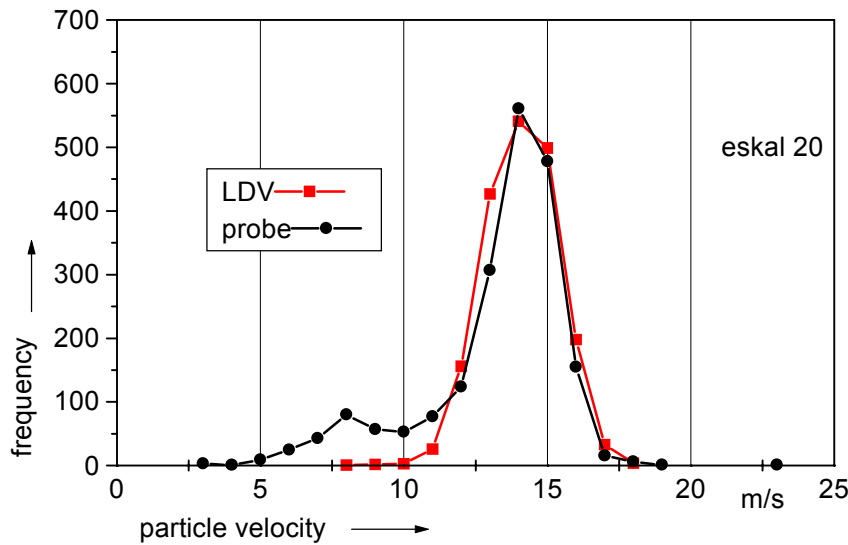


Figure 13. Frequency distributions of limestone particle velocities for eskal 20 measured by probe and LDV

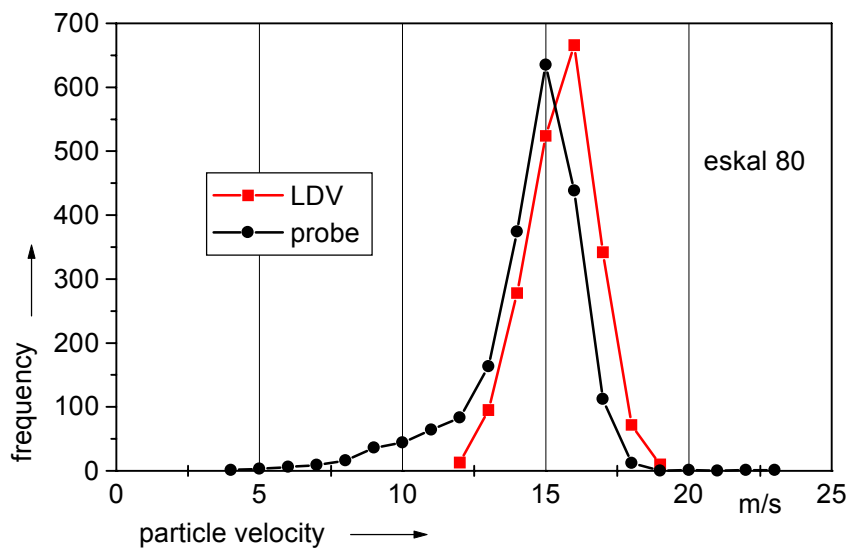


Figure 14. Frequency distributions of limestone particle velocities for eskal 80

## 5. CONCLUSIONS

The probe system based on a modified spatial filtering technique is suitable for the simultaneous measurement of particle size and velocity in multiphase flows. Measurements with test particles show a  $x_{3,50}$ -difference in dependence of the measuring range 30...1000  $\mu\text{m}$ : about 3 % for  $x \geq 100 \mu\text{m}$  and an increasing difference for smaller particles up to 10 % for  $x = 30 \mu\text{m}$ . Compared with LDV results the particle velocity values show a decreasing of the mean velocity of about 6 % and an increased standard deviation. The probe system based on a modified spatial filtering technique is suitable especially for the in-line process control in different industrial fields but also for special measurements in the laboratory.

## REFERENCIAS

- Aizu, Y. & Asakura, T. 1987 Principles and Development of Spatial Filtering Velocimetry, *Appl. Phys.*, Vol. B 43, pp. 209-224.
- Allen, T. 1997 *Particle size measurement*, 5th edn. Chapman&Hall, London.
- Feller, U., Wessely, B. & Ripperger, S. 1998 Particle Size Distribution Measurement by Statistical Evaluation of Light Extinction Signals, In *Proc. PARTEC 98, 7th European Symposium Particle Characterization, Nürnberg, Germany*, Vol. I, pp. 367-376.
- Hardalupas, Y., Hishida, K., Maeda, M. & Morikita, H. 1994 Shadow Doppler Technique for Sizing Particles of Arbitrary Shape, *Appl. Opt.*, Vol. 33, pp. 8417-8426.
- Hayashi, A. & Kitigawa, Y. 1982 Image Velocity Sensing Using an Optical Fiber Array, *Appl. Opt.*, Vol. 21, no. 8, pp. 1394-1399.
- Hussainov, M. 1999 The numerical simulation of flow of the one-point measurement flowmeter, report, Chemnitz University of Technology.
- Köser, O. & Wriedt, T. 1996 Iterative Inversion of Phase-Doppler-Anemometry Size Distributions from Sprays of Optically Inhomogeneous Liquids, *Appl. Opt.*, Vol. 35, pp. 2537-2543.
- Morikita, H., Hishida, K. & Maeda, M. 1995 Measurement of Size and Velocity of Arbitrarily Shaped Particles by LDA Based Shadow Image Technique, In *Developments in Laser Techniques and Applications to Fluid Mechanics*, Springer-Verlag, Berlin, pp. 354-375.
- Morikita, H., Hishida, K. & Maeda, M. 1994 Simultaneous Measurement of Velocity and Equivalent Diameter of Non-spherical Particles, *Part. Part. Syst. Charact.*, Vol. 11, pp. 227-234.
- Morikita, H. 1996, Ph. D. Thesis, Keio University, Japan.
- Morikita, H. & Taylor, A. M. K. P. 1998 Application of Shadow Doppler Velocimetry to Paint Spray: Potential and Limitations in Sizing Optically Inhomogeneous Droplets, *Meas. Sci. Technol.*, Vol. 9, pp. 221-231.
- Naqui, A. A. & Fandrey, C. W. 1997 Phase Doppler Measurement of Irregular Particles and Their Inversion to Velocity-resolved Size Distributions, In *Proc. Fluids Engineering Division Summer Meeting*, Vancouver, Canada.
- Onofri, F., Blondel, D., Grehan, G. & Gousbet, G. 1996 On the Optical Diagnosis and Sizing of Spherical Coated and Multilayered Particles with Phase-Doppler Anemometry, *Part. Part. Syst. Charact.*, Vol. 13, pp. 104-111.
- PARSUM GmbH 1999, Documentation of IPP30 and IPP50, Chemnitz, Germany
- Petrak, D., Rosenfeld, K. & Przybilla, E. 1996 Optical Sizing of Particles for Measurements in Processes, In *Proc. 5th GALA Conference Laser Based Methods of Flow Measuring Technique*, Shaker-Verlag, Berlin, pp. 32.1-32.5.
- Petrak, D., Rosenfeld, K. & Przybilla, E. 1998 Measurement of Size and Velocity of Particles by Optical based Spatial Filtering Technique, *9th International Symposium on Applications of Laser Techniques to Fluid Mechanics*, Lisbon, Portugal.
- Sachweh, B., Heffels, C., Polke, R. & Rädle, M. 1998 Light Scattering for In-Line Measurement of Mean Particle Sizes in Suspensions, In *Proc. 7th European Symposium Particle Characterization, Nürnberg*, Vol. II, pp. 635-644.
- Schneider, M. & Hirleman, E. D. 1994 Influence of Internal Refractive Index Gradient on Size Measurement of Spherically Symmetric Particles by Phase Doppler Anemometry, *Appl. Opt.*, Vol. 33, pp. 2379-2388.
- Witt, W. & Röthele, S. 1998 In-line Laser Diffraction with Innovative Sampling, In *Proc. 7th European Symposium Particle Characterization, Nürnberg*, Vol. II, pp. 611-624.
- Wriedt, T., Manasse, U. & Bauchhage, K. 1993 Deconvolution of PDA Size Distributions from Sprays of Optically Inhomogeneous Liquids, In *Proc. SPIE*, Vol. 2052, pp. 137-143.